ACTA STEREOL 1998; 17/3: 309-314
ORIGINAL SCIENTIFIC PAPER

CONNECTIVITY EVOLUTION OF 2D RANDOM DISTRIBUTIONS OF DISKS AND ELLIPSES: APPLICATION TO POLYPHASIC CRYSTAL ROCK DISTRIBUTION

Stéphane Sammartino[1,2], Paul Sardini[1], Eric Moreau[2], and Gérard Touchard[2]

[1]Laboratoire Hydrogéologie, Argiles, Sols et Altérations, UMR 6532, Université de Poitiers, 40 avenue du recteur Pineau, 86022 Poitiers Cedex, France.
[2]Laboratoire d'Etudes Aérodynamiques, UMR 6609, Université de Poitiers, 40 avenue du recteur Pineau, 86022 Poitiers Cedex, France.

ABSTRACT

The ultimate goal of this work is to characterise the arrangement of mineral phases using 2D images. Three simple indices are defined in order to quantify their 2D connectivity and spatial distribution. Ultimate eroded construction is used to model grain clusters. First, Monte-Carlo simulations of 2D random images permit the testing of index sensitivity to the surface area fraction, the shape and the distribution of particles in terms of the percolation threshold. This allows us to define three normalised indices for rock phase characterisation. The results are in good agreement with the morphological characteristics of the studied granite phases. They permit a comparison and a quantification of the 2D spatial arrangement of the phases which are under the percolation threshold.

Key words: connectivity, spatial distribution, random images, rock mineral phase.

INTRODUCTION

The spatial arrangement of minerals in igneous rocks such as granite results from the crystallisation processes that occur during rock genesis. Thus, it is of very high importance for the location and the connectivity of the microporosity to quantify the mineral spatial arrangement. The study of these rock properties, which control the transport and the alteration processes, extends to many practical applications such as geothermal energy extraction and nuclear waste deposit. The aim of this paper is to define and to test simple indices in order to characterise the spatial arrangement of mineral phases using 2D-images.

Mineral phases are composed of crystals that are 3D convex entities. In the present 2D-image analysis, we have defined a grain to be a 2D section of a crystal and a cluster to be a set of adjacent grains of the same mineral phase. Thus, the 2D-image of a mineral phase is composed of grains and clusters which are called particles. They can be convex or non-convex (Coster and Chermant, 1989). The question then is how to locate grains in non-convex particles on 2D-images of core sections. We have chosen to treat this problem using the concept of ultimate eroded (UE) construction. The UE determination in a non-convex particle is based on the fact that each of its convex part gives one UE (Coster and Chermant, 1989).

Thus, in order to isolate grains in a particle, we reduce each convex part to its corresponding UE. Obviously, this approach is only a means of modelling grains in particles in 2D-images. This method represents the first step of the separation particle algorithm of Jernot (1982). Based on this concept of particles and grains located by UE construction, three global indices are defined and then used to quantify their spatial arrangement in two dimensions.

DEFINITION OF INDICES

Grain Clustering Index (GCI)

The *GCI* is calculated using the definition given by Sardini *et al.* (1997) (equation 1). This index quantifies the trend of grains to be clustered and varies from zero for an image without any cluster (one grain per particle) to unity for many grains in few particles. It gives no information about the distribution of particles but is related to the mean number of grains per particle:

$$GCI = 1 - \frac{N_P}{N_G} \tag{1}$$

Here N_P is the number of particles and N_G the number of grains determined by the UE construction.

Spatial Distribution Index (SDI)

The *SDI* is based on the calculation of the mean distance $\overline{D}$ between the centre of grains and their nearest neighbour (equation 2). The distance between each grain is assumed to be the distance between their corresponding UE. This mean distance determined for all grains is then normalised by the theoretical same mean distance for a random distribution of points D_p, where the number of points is equal to the number of UE (Coster and Chermant, 1989). Hence, the *SDI* is given by equation 3 (Jerram *et al.*, 1996).

$$\overline{D} = \frac{\sum_{1}^{N} d_i}{N_G} \tag{2}$$

$$SDI = \frac{\overline{D}}{\overline{D_p}} \tag{3},$$

where d_i is the distance between the centre of the i^{th} grain to its nearest neighbour.

This index has shown to be useful for the determination of the spatial distribution of points, suggesting that:

- $SDI = 0$ if all points are at the same position,
- $SDI = 1$ for a random distribution,
- $SDI < 1$ for a clustering/chaining distribution,
- $SDI > 1$ for an ordering distribution.

Chaining Connectivity Index (CCI)

The *CCI* is a directional index determined by a double geodesic propagation in an octagonal graph. This index is related to the speed of propagation of fluids through the rock assuming that is less though the matrix than through some specific rock phase (Sardini *et al.*, 1997). This provides a means of quantifying the ability of a phase to create an efficient flow path.

Two linked propagations with different velocities take place in the two phases, the matrix phase (white colour) and the studied phase (black colour) (Fig. 1a).
The method of double propagation is defined as follows:

- A propagation front (grey colour on the Fig. 1a) is placed on the top of the image, the propagation cycle number (*PCN*) is equal to zero.
- This front is dilated (Figs. 1b, c). When it reaches a particle, this is instantaneously overgrown.
- The propagation is stopped when the front attains the bottom of the image (Fig. 1d).

The final value of the *PCN* corresponding to the number of dilations required to cross the image perpendicular to its height (*H*), permits the calculation of the *CCI* using equation 4. It mainly depends on the distance between each cluster in this direction:

$$CCI = 1 - \frac{PCN}{H} \qquad (4)$$

This index varies from zero to unity. $CCI = 0$ if $PCN = H$ means that there is no particle present and $CCI = 1$ if $PCN = 0$ means that the studied phase creates an infinite cluster between the top and the bottom of the image. Thus, this index is related to the notion of the percolation through the image. If $CCI = 1$, the phase is above the percolation threshold (Sahimi, 1995).

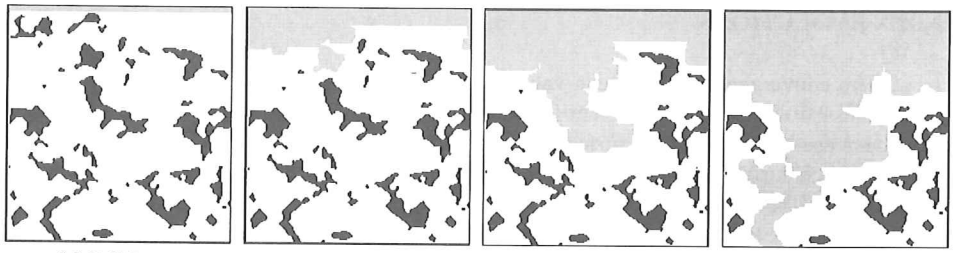

(a) PCN = 0 (b) PCN = 10 (c) PCN = 20 (d) PCN = 30

Fig. 1. Example of the double propagation method for the determination of the CCI *on an isolated rock phase in a matrix.*

2D SIMULATED RANDOM IMAGES

Random images of particles are used to simulate an isolated mineral phase in a 2D-image. This permits the testing of sensitivity indices to the surface area fraction and the shape of particles in terms of the percolation threshold. The fact that the simulated images are random provides a reference in determining the spatial arrangement in real mineral phases.

Firstly, points are uniformly located on an image according to Poisson's model (Coster and Chermant, 1989). Secondly, grains are created from each point and can interpenetrate according to the Boolean model to form particles. Three types of distribution on square images (500×500 pixels) are generated:

- Type I: random distribution of disks with a diameter of 20 pixels (Fig. 2a),
- Type II: random distribution of disks with a uniform diameter distribution through the range of 6 to 40 pixels (Fig. 2b),
- Type III: random distribution of ellipses with a main axis of 20 pixels. The orientation and the ellipticity are random (Fig. 2c).

The sizes of disks and ellipses correspond to the width of rock grains determined by successive openings. On average for the three phases of interest, the size of grains is less than 40 pixels. Their mean value is about 20 pixels. As shown in Fig. 2, these three types of image simulate a varying complexity of particles.

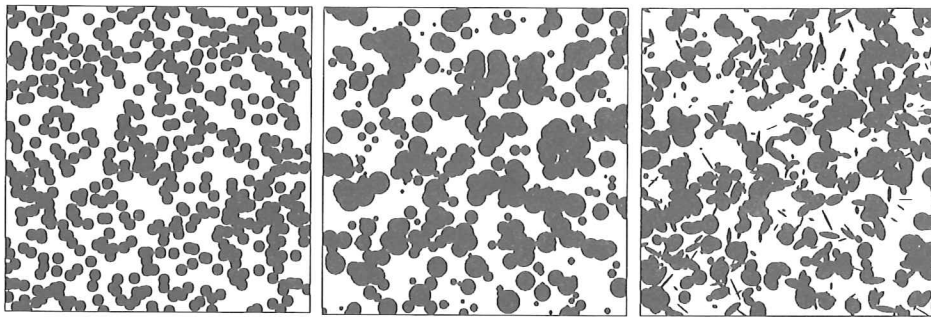

(a) Type I (b) Type II (c) Type III

Fig. 2. Example of the three types of simulated images. The surface area fraction is 50 %.

INDEX EVOLUTIONS

The convergence of the mean value of each index is tested over a set of 100 images. Nevertheless, 50 images are sufficient for an accurate index determination. Standard deviation errors decrease quickly with the surface area fraction excepted for the *SDI* (Fig. 3c).

At each surface area fraction, the percolation probability is given by the percentage of images above the percolation threshold using *CCI*. As shown in Fig. 3a, the percolation threshold is lower for the random distribution of ellipses (type III). Thus, the grain anisotropy seems to be important in the 2D-connectivity of the phase (Fig. 3a). The percolation threshold of type II distribution is greater than those of type I even though the fixed diameter of the type I distribution (20 pixels) is less than the mean diameter of the type II distribution (29 pixels). This means that the size homogeneity seems to favour the 2D-connectivity compared to a size distribution. This is due to the smallest particles which have little influence on the phase connectivity.

Indices mainly depend on the surface area fraction (Fig. 3b, c, d). The *GCI* behaviours are almost linear below the percolation threshold. The effect of a random particle size (type II and III) is to decrease the slope value. This is induced by the small particles isolated in the matrix phase (Fig. 3b). As shown in Fig. 3c, the *SDI* curves show a slight variation in terms of the surface area fraction in spite of the fact that the particles become more connected. This may be related to the grain determination by UE. The type of distribution does not influence the *CCI*. It is more sensitive for the lowest surface area fractions. In summary, these indices do not indicate significant variations in terms of the three distribution types. The *GCI* and the *CCI* strongly depend on the surface area fraction. Therefore, for a comparison of real phases, they need to be normalised. The *SDI* is not useful for this type of Boolean model. It was only used on images of discernible grains or points distribution (Jerram *et al.*, 1996), so it is strongly depending on the UE construction. Consequently, we have chosen to use three normalised indices for the study of real mineral phases.

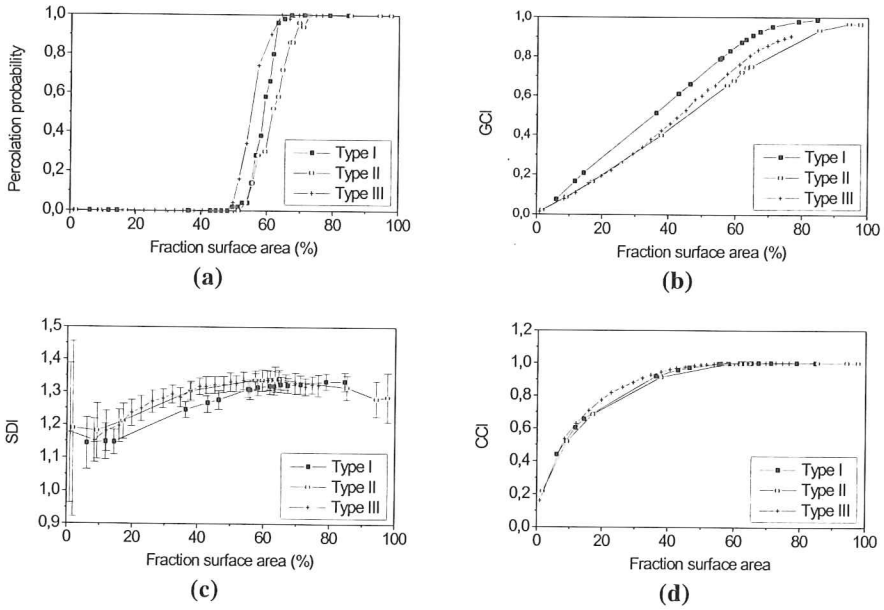

Fig. 3. (a) Percolation probability and (b) (c) (d) index behaviours in terms of the surface area fraction for each type of simulated images.

The *GCI* and *CCI* values of real phases are subsequently normalised by the values determined on type I image at the same surface area fraction. The *SDI* index will be calculated by the ratio of the distances $\overline{D}$, determined on real phases and on simulated type I images, without taking into account the distance $\overline{D_p}$. Normalisation is used to avoid the influence of the surface area fraction and the UE construction on index values.

APPLICATION TO POLYPHASIC CRYSTAL ROCKS

The three major phases of the studied granite are thresholded using a specific staining method of core sections (Sammartino *et al.*, 1998) and an in house software package (Sardini, 1996). The rock is composed of a feldspar phase (white colour) which is above the percolation threshold. The two other phases are dark minerals (black colour) and quartz (grey colour) (Fig. 4a). The quartz phase has proved to contain a more important population of small particles than the dark mineral phase. As shown in Fig. 4b, the *GCI* values outline a clustering distribution of dark minerals and quartz crystals. The dark mineral crystals are more clustered than the quartz crystals. This is induced by isolated quartz grains in the feldspar phase (Fig. 4a). The *GCI* values are in agreement with the *SDI* values that indicate a clustering/chaining distribution. The *CCI* values for the dark mineral and quartz crystals are similar. This shows the slight influence of the isolated quartz crystals on the *CCI* determination and is in agreement with their nearly similar *SDI* values. The *GCI* and *CCI* values of the feldspar phase give no useful information. Nevertheless, the *SDI* value close to unit highlights a random distribution of the feldspar crystals.

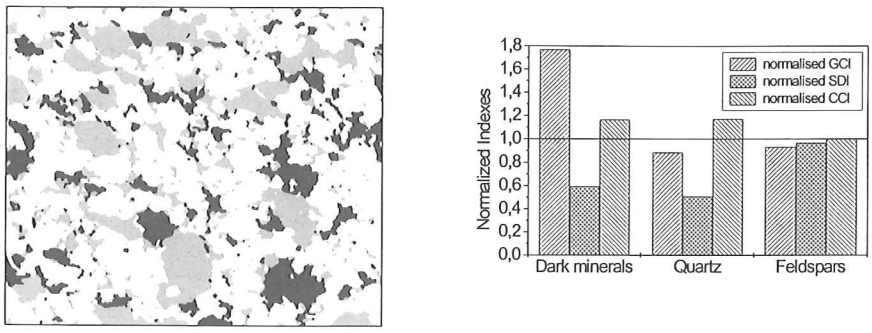

(a) (b)

Fig. 4. (a) Example of the spatial distribution of the studied mineral phases. (b) Normalised indices for the three major phases of a granite.

CONCLUSION

The results are in good agreement with the morphological characteristics of the studied granite phases. Indices give a comparison and a quantification of their 2D spatial arrangement. But, they are only useful for the phases which are under the percolation threshold. This means of investigation should provide interesting results on the majority of igneous rocks.

Obviously, the relationships between two and three dimensions are still unknown as 2D images can not fully represent the 3D-structure of the rock. Hence, this work constitutes a simple means of comparing mineral phases using 2D images and to extend our knowledge of this rock type. This is in keeping with the recent investigations undertaken in our laboratory (Moreau *et al.*, 1996).

REFERENCES

Coster M, Chermant JL. Précis d'analyse d'images. Presses du CNRS, 1989.

Jernot JP. Analyse morphologique et modélisation du frittage et des matériaux frittés, thèse de l'Université de Caen, 1982.

Jerram DA, Cheadle MJ, Hunter RH, Elliott MT. The spatial distribution of grains and crytals in rocks, Contrib Mineral Petrol, 1996, 125 : 60-74.

Moreau E, Sardini P, Touchard G, Velde B. 2D and 3D morphological and topological analysis of a clay soil, Microsc. Microanal. Microstruct., 1996, 7 : 499-504.

Sahimi M. Applications of Percolation Theory. Taylor & Francis. 1995.

Sammartino S, Touchard G, Meunier A, Patrier P. Etude de la microperméabilité des roches granitiques du site Sud-Vienne, rapport ANDRA n°316 406 A0, 1996.

Sammartino S, Sardini S, Moreau E, Touchard G. Morphologie et connexité 2D sur trois faciès d'altération diffuse de tonalite, présentation orale ISS, Ecole des mines de Paris, 1998.

Sardini P, Ledésert B, Touchard G. Quantification of microscopic porous networks by image analysis and measurements of permeability in the Soultz-sous-Forêt granite. Fluid Flow and Transport in Rocks. Chapman & Hall. 1997, 171-188.

Presented at the 7th European Congress for Stereology, Amsterdam, April 20th to 23rd, 1998.